

# Tests of Useful Field of View of Laser Sensors Used in Autonomous Nano Sumo Robots

Mateusz Świącki, Józef Szymelewicz, Jerzy Matusiewicz, and Rafał Grądzki

Faculty of Mechanical Engineering, Białystok University of Technology, Białystok, Poland  
Email: mateo960@gmail.com, drzozef@wp.pl, j.m.oficjalny@gmail.com, r.gradzki@pb.edu.pl

**Abstract**—The article aims to compare two sensors for the possibility of their use in autonomous designs of NanoSumo class robots. The tests were carried out for FOV (field of view), which is a useful detection field. For this purpose, a measuring stand was built, whose operation consisted of moving two screens in two perpendicular axes. The screens are moved in the X-axis to a maximum distance of 50 mm and can be moved to a maximum distance of 172 mm. Lengths have been selected so that they correspond to the ring on which the robot moves. The sensors have also been taken into account as the width of their field of view at the maximum measuring distance does not exceed 50 mm. A white sheet was used as a measuring surface to obtain the best possible results. Finally, the sensors were compared in terms of their FOV. Recommendations on the selection and placement of sensors in the robot are also presented.

**Index Terms**—Autonomous robot, sumo robot, sensor, navigation, control

## I. INTRODUCTION

A mobile robot needs a proper control system to be able to move around in a given work environment. It must, thanks to the information provided by the sensors, properly control executive devices such as motors, manipulators, etc. The more accurate a sensor is and the more data it provides, the more valuable it is and can be used for more complex operations. The programmer creating an algorithm to control the robot has many more possibilities thanks to such information, and the code itself can be better optimized and faster. [1]-[4]

In the case of not very complex navigation systems, laser sensors are commonly used to measure the distance from an obstacle to the position of the robot. Such sensors allow creating a map of the environment. They are used in robots responsible, for example, for cleaning at home or delivering things. [5]-[7]

Laser sensors are usually better than infrared sensors, due to the broader measuring range. However, if the workspace of a given robot is not large, they can be used interchangeably, as the measurement and processing speed of both types of sensors are similar. [8], [9]

The sensors use three measurement methods: triangulation method, interference method, and real-time (time-of-flight) measurement. The triangulation method uses angles in a triangle. The first apex of the triangle forms a beam of light reflected from the object, while the other two belong to the sensor transmitter and receiver.

The distance is determined by measuring the angles of the triangle or by measuring the length of the triangulation base. In both cases, a simple mathematical formula is used to calculate the distance value. The interference method uses overlapping monochromatic waves (usually laser light) of the same frequency but different amplitudes and phases. After these overlapping waves, a different monochromatic wave of the same frequency is created, but other factors are different. Using the interference equation, you can calculate the distance from the measured object. The last method is the time of flight. It is the simplest method because it uses the time of light travel from the transmitter to the receiver and on this basis the distance from the object is calculated. For this reason, the receiver and the transmitter are placed very close to each other, which makes the sensors very compact and shading effects are avoided. However, they require a precise clock, as the speed of light makes the time of the waveform from the transmitter to the receiver very low. [10]

Infrared sensors are not as versatile as laser sensors, because their reaction depends on the reflection characteristics of the detected object. This is the reason why these sensors are used in robotics to detect and bypass obstacles. However, their fast response time is a very beneficial factor that makes this type of sensors widely used to improve the vision system of a mobile robot for real-time operation and to map the environment in which the robot moves. [11]

Each sensor has different parameters. They are often described in the technical documentation. Basic parameters describing the sensor:

- resolution - the smallest physical change that can be recognized by the sensor,
- Non-linearity error - the most significant deviation of the actual value from the measured one,
- measuring range - this is the range of values measured by the sensor which do not exceed the permitted limit error (between measured and actual value),
- sensitivity - the effect of input value change on output value change.

The article focuses on the measurement system for the nano sumo robot. The purpose of this robot is to fight with other such devices in the ring. The robot that pushes the opponent out wins the fight. The ring for this type of

robot has a diameter of 192.5 mm. The robot's dimensions are within 25 x 25 x 25 mm, and its weight does not exceed 25 g. Due to the small size of the robot, the selected sensors must be as little as possible.

To construct a good measurement system, tests were performed to determine the angle of view of each of the tested sensors under conditions corresponding to the real combat conditions of nano sumo robots. Based on the measurement data, visualizations of various configurations of sensor settings were prepared and compared with each other.

## II. RESEARCH METHODOLOGY

### A. Tested Sensors

There are many laser distance sensors available on the market, but many of them are too large to be used in nano sumo robots. Sensors meeting dimensional requirements often do not offer a sufficient measuring range and are not suitable for the robot's navigation system. In the tests, sensors were selected that meet the requirements for dimensions (it is possible to place more in the constellation), measuring range, and measuring speed.

Two sensors were selected and tested for further research: Pololu 2490 - VL53L0X and Pololu 2489 - VL6180X. Their parameters are shown in Table I, based on catalogue data.

TABLE I. TESTED SENSORS [12], [13]

	Pololu 2490 - VL53L0X	Pololu 2489 - VL6180X
Supply Voltage	2.6 V to 5.5 V	2.7 V to 5.5 V
Working range	0 - 2000 mm	0 - 100 mm
Light source	Red LED	850 nm laser
Response time	8 - 200 ms - depends on measurement mode (standard - 33 ms)	max. 19 ms
Dimensions (L x W x H)	13 mm x 18 mm x 2 mm	13 mm x 18 mm x 2 mm
Price	9.95 \$	8.49 \$

Pololu 2490 - VL53L0X (Fig. 1) is quite an advanced sensor that guarantees measurements not only of distance but also of light intensity. It uses a time-of-flight measurement method. This means that the laser triangulation method is not used here, but the measurement of the time from the infrared laser pulse to its return to the detector. It contacts the master device using the I2C bus. It has a measuring range that goes far beyond the dimensions of the NanoSumo robot fight ring, but its price is higher.



Figure 1. Pololu 2490 - VL53L0X sensor. [14]

Pololu 2489 - VL6180X (Fig. 2) works on the same principle and uses the same communication method as the previously described sensor. The only differences are a smaller measuring range and lower price.



Figure 2. Pololu 2489 - VL6180X sensor. [15]

The artwork focuses on determining the useful field of view of the previously described sensors. The information obtained can be used in designing navigation systems for mobile robots. It will then be possible to optimize the number of used sensors so that their number is as small as possible. This will enable the costs of the sensors themselves to be minimized, make a more straightforward design and less load on the processor supporting the navigation system control.

### B. Research Station and Measurement Methodology

To test the sensors for their useful field of view, a measuring stand was made (Fig. 3).

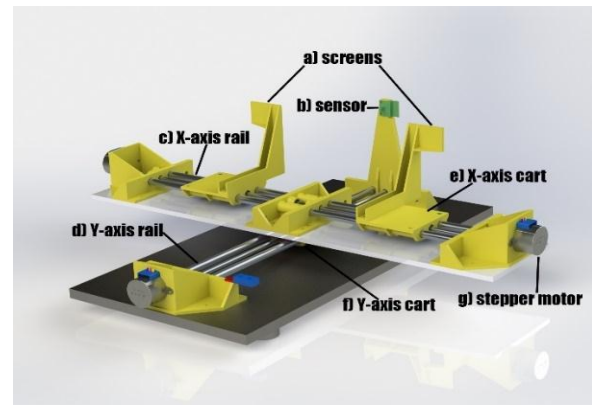


Figure 3. Research station: a) screens, b) sensor, c) X-axis rail, d) Y-axis rail, e) X-axis cart, f) Y-axis cart, g) stepper motor.

The workstation operates by positioning two screens with different surfaces in x and y axes. This is achieved by means of two rails arranged perpendicularly to each other, which are constructed of two aluminium tubes leading a plastic cart. The longitudinal movement of the carts is possible thanks to the screw and the motor, which is responsible for turning the screw and thus moving the cart. This solution allows for more precise positioning of the carts, especially since the changes in their position between individual measurements are small and greater precision is required. The sensor is permanently located at the front of the test bench, which will be approached by two identical screens placed on the same rail. The size of the screen that the sensor can detect is 25 x 37 mm.

The maximum distance to which the screens can be moved away from the sensor is 172 mm. The maximum distance between the screens and the centre point is 5 cm. The step of the cart in the x-axis is 4 mm, while in the y-axis it is 0.5 mm. The sensors and motors are powered by a contact plate and an Arduino Uno board, which will be responsible for recording the measurements and saving them to file later. The same microcontroller plate will realize the algorithm that controls the motors for screwing.

The above tests will make it possible to determine the FOV of the sensor by checking whether the screens are detected and whether the result of the distance returned by the sensor is accurate. Additionally, their effectiveness will be studied by changing the surface on the screens. The distances are not too long, as they are adjusted to the conditions in which nano sumo robots fight (the ring has a diameter of 192.5 mm).

### C. Measurement Algorithm

The measurement algorithm is presented in graphical form in Fig. 4. The procedure of starting the measurements starts from:

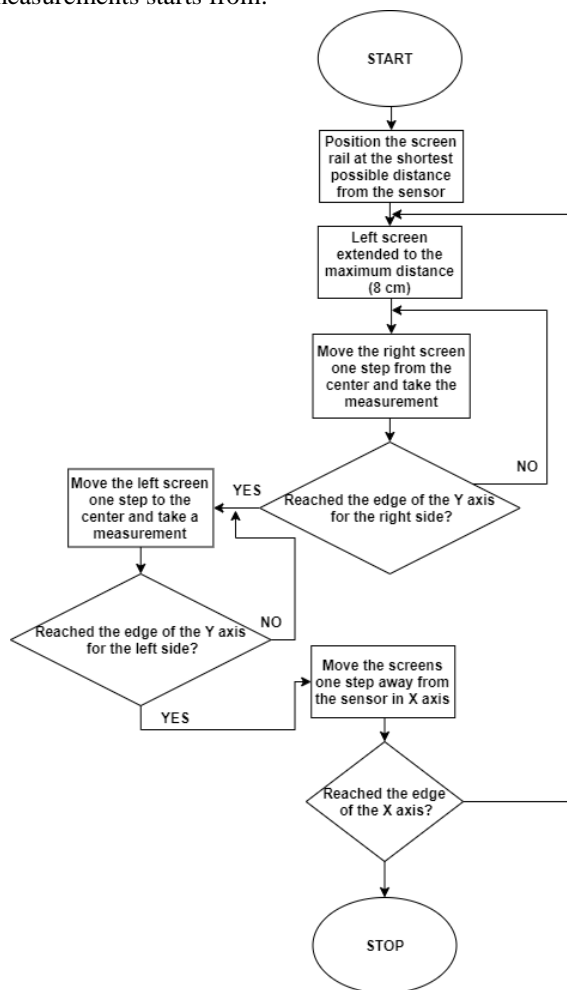


Figure 4. Measurement algorithm.

1. Set the screen rail to the shortest possible distance from the sensor.

2. The left screen is extended to the maximum distance (50 mm).
3. Move the right screen one step from the centre and take the measurement.
4. Execution of point 3 until reaching the y-axis edge.
5. Move the left screen one step in and take a measurement.
6. Perform point 5 until you reach the centre of the y-axis.
7. Move the screens one step away from the sensor.
8. Perform points 2-7 up to the end of the x-axis range.

### III. PRESENTATION OF THE RESULTS

The measurements were taken on screens with a white card glued to them. White surfaces reflect the most significant amount of light, so these are the best conditions for the tested sensors. [1]

#### A. Presentation of Measurements on the 2D Chart

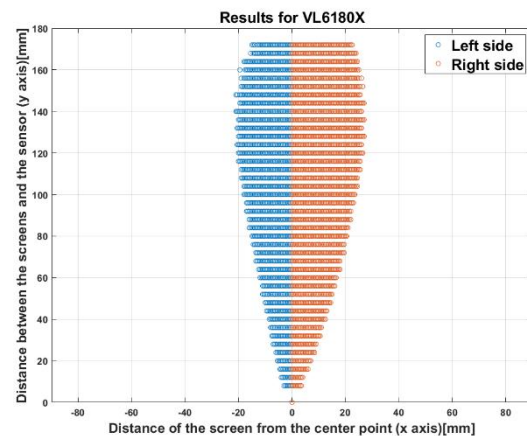


Figure 5. Measurements for VL6180X.

The VL6180X laser sensor (Fig. 5) has a linear relationship between the viewing range and the viewing width up to 120 mm. Over a longer distance, the sensor's field of view is narrowed. This may be since the sensor is designed for distances up to 100 mm. There is also an asymmetry in the width of the sensor's field of view, namely the right field of view is wider than the left.

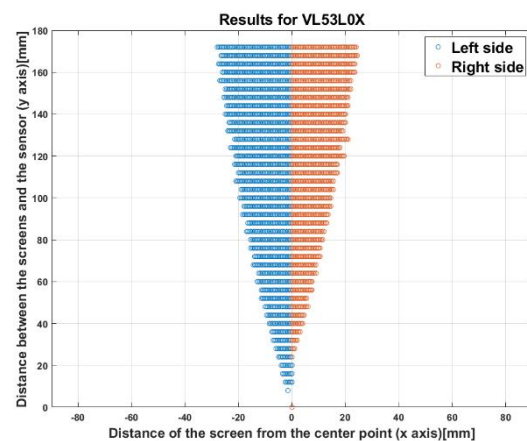


Figure 6. Measurements for VL53L0X.

The VL53L0X laser sensor (Fig. 6) has a reasonably regular viewing cone. On the left side, there are larger values on the x-axis than on the right side, which means better visibility. This is the opposite of the sensor described above. As the screen is moving away from the sensor, its viewing width expands to the maximum value of 28 mm on the left side and 24 mm on the right side (the distance from the screen is 172 mm). There is no detection of the right screen for small values of the distance between the sensor and the screen.

In both cases, the measurements show a certain asymmetry, consisting of shifting the cone of vision in one direction. The reason is the construction of sensors because the light receivers are located at the side edges of the housing. When measuring the VL53L0X, the receiver was close to the left edge of the casing (Fig. 7), while for the VL6180X it was close to the right edge (Fig. 8).

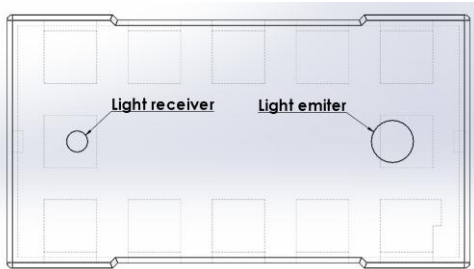


Figure 7. VL53L0X sensor housing.

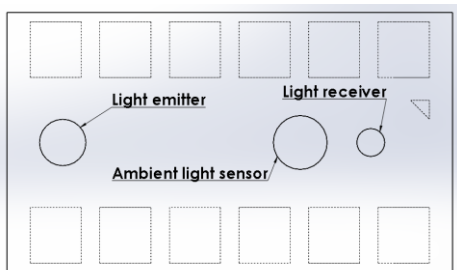


Figure 8. VL6180X sensor housing.

**B. Presentation of the Vision Angle Width Measurements**

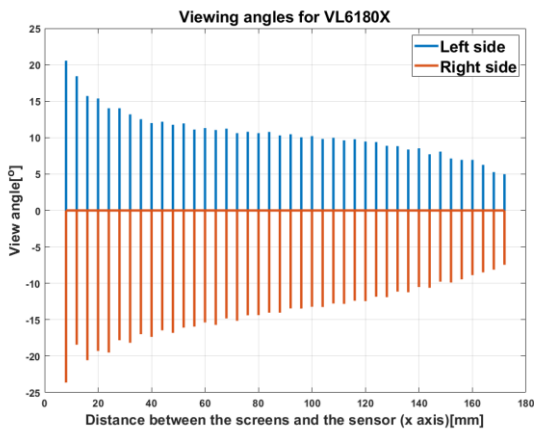


Figure 9. Viewing angles for the sensor VL6180X.

With the VL6180X sensor (Fig. 9), it can be seen that the most extensive viewing angles occur at the shortest distances between the screens and the sensor. They are maximum 21 °for the left side and 23 °for the right side. The smallest viewing angles are at the end of the X axis. They are 5 °for the left side and 8 °for the left side. The viewing angles for the left side decrease rapidly to about 50 mm of the screen distance from the sensor. Then the angle decreases slightly to a distance of about 124 mm from the screens. Then again, there is a sharp decrease until the end of the range. For the right side, however, the angle drop is constant over the entire range and not as sharp as for the left side.

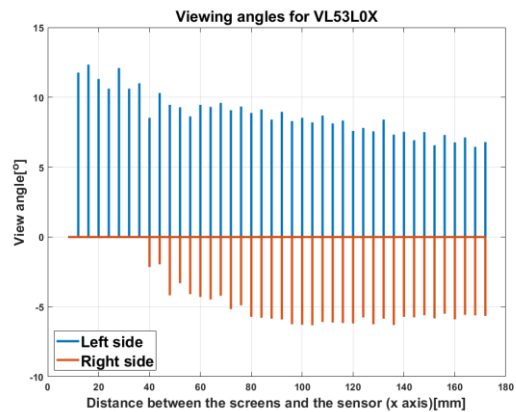


Figure 10. Viewing angles for the sensor VL53L0X.

With the VL53L0X (Fig. 10), the widest viewing angles, as with the previous sensor, can be seen at the beginning of measurements. They are only visible on the left side. They are a maximum of 16 ° For the left side, the angles decrease quite steadily as the distance between the screens and the sensors increases to a minimum value at the end of the range. The minimum value is 7 ° For the right side, to the value of 36 mm of the distance between the screens and the sensor, the angle is 0 °. It results from the asymmetry of the viewing cone shown in Fig. 6. Then the value of the angle increases to about 72 mm of the distance. Then the angle value remains relatively constant until the end of the measuring range. The maximum angle value for the right side is 6 ° and is 100 mm from the beginning of the X axis range.

**IV. VISUALIZATION OF THE CONFIGURATION OF SENSOR SETTINGS IN THE ROBOT**

Based on the described measurements, visualizations of various configurations of sensor settings in the NanoSumo robot were created using two tested sensors and compared with each other.

**A. The Parallel Setting of Two Sensors**

In the parallel configuration, the two VL53L0X sensors (Fig. 11), whose centres are 9 mm apart, have two viewing cones. This configuration allows you to detect the position of the opposite robot. A signal from two sensors means that the opponent is in front of the robot. However, a signal from only one sensor means that

the obstacle is in the left or right part of the robot's detection area.

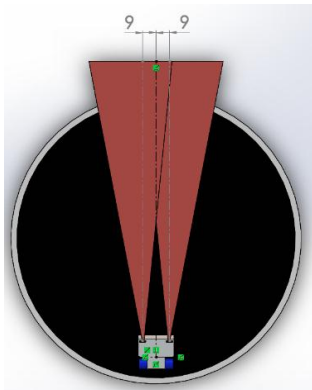


Figure 11. Configuration of the two sensors VL53L0X in parallel.

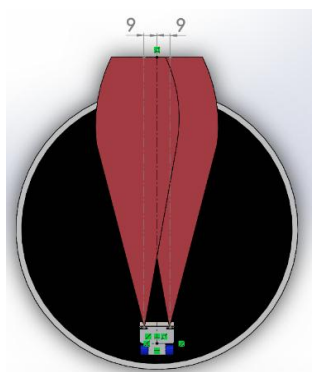


Figure 12. Configuration of the two sensors VL53L0X in parallel.

The same configuration for the VL6180X (Fig. 12) also has two sensors 9 mm apart. It has similar features to the format described above, but it differs from the previous one with wider visibility cones. This is a sure advantage of these sensors over the previous ones described in this configuration.

In the course of research on the above sensor settings, it was observed that a 180° change in sensor orientation has an impact on the position of sensor cones. This change is shown in Fig. 13 and Fig. 14.

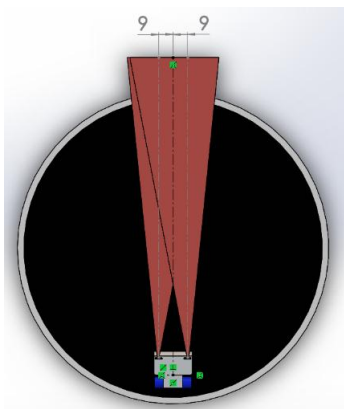


Figure 13. Configuration of the two sensors VL53L0X in parallel (reorientation).

The positions of the vision cones are changing and descending more closely inwards. This means a more

narrowed field of vision, compared to the previous configuration.

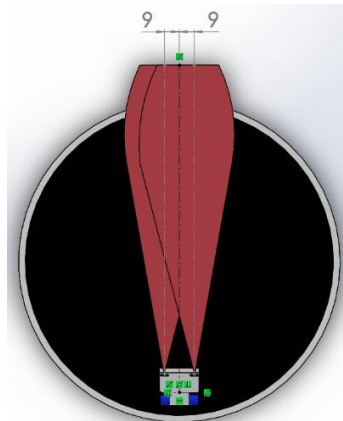


Figure 14. Configuration of the two sensors VL6180X in parallel (reorientation).

### B. Two Sensors Beveled

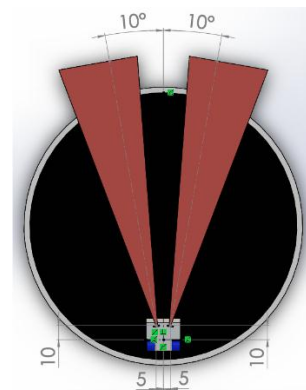


Figure 15. Configuration of two sensors VL53L0X set up diagonally.

When two VL53L0X sensors are configured diagonally (Fig. 15), the viewing cones are inclined by 10° from the vertical axis. In this configuration, the sensors provide a wider field of view, but there is a dead zone between the two sensor cones. It may be unfavourable at greater distances because the angle of this zone starts to increase. At small distances, the problem becomes invulnerable because the opponent will then cover one of the cones. The problem with this configuration is whether the obstacle is in front of the robot.

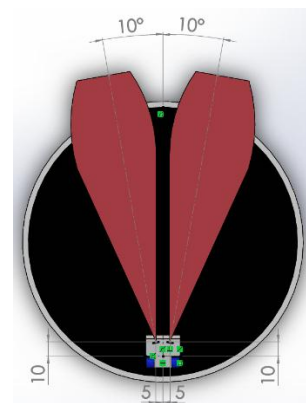


Figure 16. Configuration of two sensors VL6180X set up diagonally.

The VL6180X in this configuration with Fig. 16 provides a smaller dead zone than the previously described sensors. However, the dead zone is still present, and as the sensor has problems with detection beyond 10 mm (then it depends on the ambient conditions), the dead zone can be much longer at further distances than the VL53L0X. However, in the ring to NanoSumo, this is not a problem.

C. Three Sensors Beveled

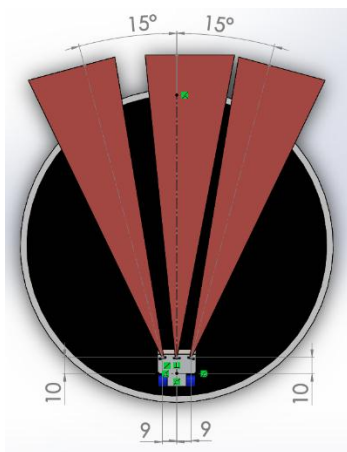


Figure 17. Configuration of three sensors VL53L0X set up diagonally (first version).

In the configuration of the arrangement of the three sensors VL53L0X (Fig. 17), one can see that gaps in the field of view are formed. The slot on the left may not be a problem, while the larger slot may cause the robot not to see the enemy for a while. This is a significant drawback of the robot's vision system.

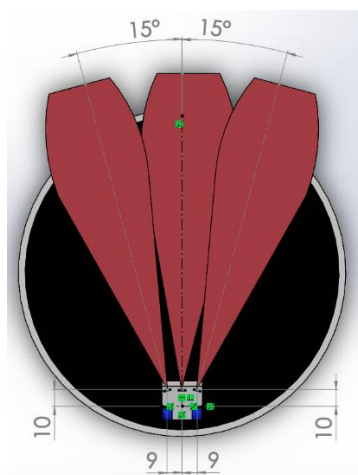


Figure 18. Configuration of three sensors VL6180X set up diagonally (first version).

In the configuration of the position of three VL6180X sensors (Fig. 18), one sensor is positioned in the middle of the robot facing straight. The side sensors are at the same height, 9 mm apart and 15 degrees offset. In this configuration, the robot's field of view is as complete as possible, and the fields of view of the individual sensors overlap. Therefore, it is not possible to overlook the enemy.

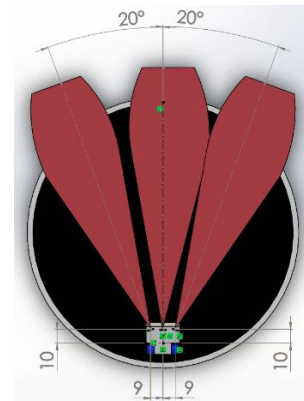


Figure 19. Configuration of three sensors VL6180X set up diagonally (second version).

The configuration of the VL6180X sensors (Fig. 19) is similar to the one described above (Fig. 18). The only difference is the position angle between the sensors, which is 20 degrees. This configuration shows once again the advantage of the VL6180X because its fields of view cover the space in front of the robot better than the VL53L0X.

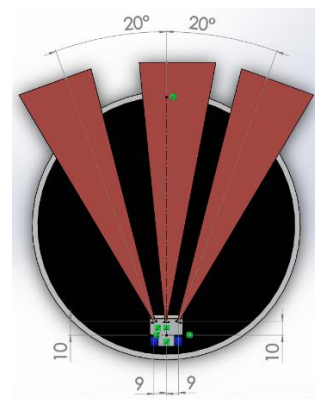


Figure 20. Configuration of three sensors VL53L0X set up diagonally (second version).

The configuration of the VL53L0X sensors (Fig. 20) is set as described earlier (Fig. 19). It shows gaps in the field of view of the sensors with considerable width. The advantage of this permutation is quite a wide field of view compared to the combination of two sensors.

D. Four Sensors Beveled

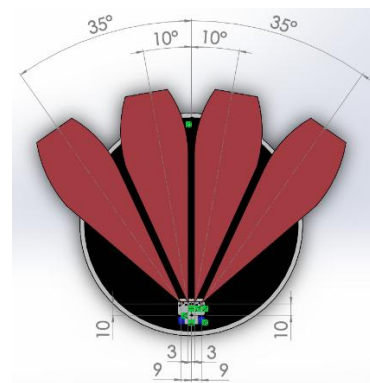


Figure 21. Configuration of four sensors VL53L0X set up diagonally.

The combination of the four sensors VL6180X (Fig. 21) shows how wide an area can be observed with four sensors without leaving large gaps between the individual sensor fields of view. The critical issue here is the symmetry of the field of view, which did not occur with three devices.

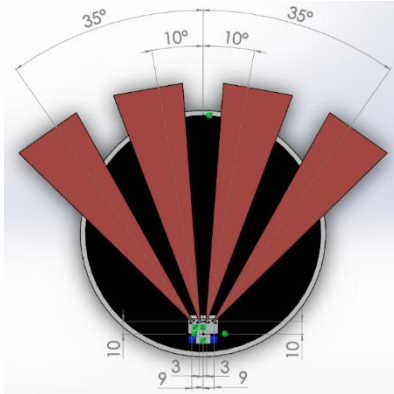


Figure 22. Configuration of four sensors VL53L0X set up diagonally.

The configuration of the four VL53L0X sensors (Fig. 22) has been set as described in the previous configuration (Fig. 21). Despite the large width of the field of view, there are much larger blind spots than with the VL6180X. This also means that to get a similar field of view with the VL53L0X (Fig. 21), it is necessary to use more sensors. Such a procedure causes technical and programming difficulties.

## V. SUMMARY AND CONCLUSIONS

Thanks to the research carried out. It was possible to determine the differences between the two laser sensors. The cones of vision, which turn out to be asymmetrical, were determined due to the construction of the sensors themselves. Therefore, it is crucial to take into account the asymmetry and its ornamentation when designing to obtain the best possible area for the robot to detect obstacles.

With the VL53L0X, the viewing cone is symmetrical. In addition, it is offset to the left of the X axis. This is due to the position of the receiver in the sensor housing. The visibility cone of the VL6180X shows a similar offset for the same reason. The difference is the asymmetry of the cone that can be shown at the end of the measuring range in the y-axis as the cone begins to narrow irregularly. The VL6180X provides a wider field of view compared to the VL53L0X.

For both sensors, the widths of the viewing angles are the largest at the very beginning of the measuring range of the y-axis and the smallest at the end. Also, they are characterized by a difference in values, depending on the analyzed side. This results from the previously described sensor design.

The visualizations of the tested configurations show that the best performing arrangements are those where the sensors are at an angle to the vertical axis. There is no excessive overlapping of the individual sensors' fields of view, which makes the detection area larger. It is also easier to determine the position of the opposite robot, as

the viewing cones are separated from each other, making it easier to create code for the navigation system.

The VL6180X is best suited for these configurations because of its wider field of view. In slanted sensor positions, the sensors provide a small dead zone, which gives them an advantage over the VL53L0X. Although their field of view begins to narrow over longer distances, in a ring created for nano sumo, this is not a problem as the sensors provide sufficient detection area.

The tested sensors are characterized by small dimensions, which enable their application in constructions, where the available space is limited. In NanoSumo robots, where the allowed dimensions are tiny, such sensors can be very good at welding, because it is possible to use more of them, which expands the detection field by the robot. Similar sensors with such dimensions guaranteeing measurement in TOF technology, returning the measurement as a value of the distance from an obstacle are hard to find.

An additional advantage of these sensors is their price and availability. A massive shot characterizes the costs of laser distance sensors. Most often, with a higher price goes better precision of measurement by the sensor, but its dimensions are independent of this aspect. The tested sensors are characterized by high availability, small price, and small dimensions, which makes it easy to apply to such projects as small mobile robots.

## CONFLICT OF INTEREST

The authors declare no conflict of interest.

## AUTHOR CONTRIBUTIONS

Mateusz Świącki was responsible for writing and formatting the article, as well as processing the measurements in Matlab. Jerzy Matusiewicz created a prototype of the measurement stand and was responsible for writing parts of the article. He also prepared visualizations of sensor configuration in Solidworks. Józef Szymelewicz was accountable for creating the final version of the measuring station, including its programming on the Arduino board, and for making measurements. Rafał Grądzki was an originator of the subject of this article and coordinated the authors' work. He also assisted in the writing of these papers. All authors had approved the final version.

## ACKNOWLEDGMENT

The paper is funded by the Ministry of Science and Higher Education of Poland under the "Najlepsi z najlepszych! 4.0" program.

## REFERENCES

- [1] M. Świącki, J. Szymelewicz, J. Matusiewicz, R. Grądzki, "Tests of selected sensors applicable in autonomous mini sumo robots," *International Journal of Mechanical Engineering and Robotics Research*, vol. 9, no. 8, pp. 1145-1151, 2020.
- [2] B. Pawłowski, M. Wysocki, R. Grądzki, "Performance examination of selected sensors for use in autonomous robots," in *Proc. AIP Conference Proceedings 2029*, 020055 (2018).

- [3] M. Ł. Słowik and D. Oldziej, "Experimental verification of parameters and characteristics of the robot rangefinder," *Acta Mechanica et Automatica*, vol. 4, no. 3, pp. 124-129, 2010 (in Polish).
- [4] P. Wasilewski, K. Chojnowski, R. Grądzki, "Autocalibration of gyroscope based two-step regulator for autonomous vehicles," *MATEC Web of Conferences*, 182, 01030, 2018.
- [5] K. Chojnowski, P. Wasilewski, and R. Grądzki, "Movement modeling of mobile robot in MegaSumo category," in *Proc. AIP Conference Proceedings*, 2029, 020010, 2018.
- [6] M. H. F. M. Fauadi, S. Akmal, M. M. Ali, N. I. Anuar, S. Ramlan, A. Z. M. Noor, and N. Awang, "Intelligent vision-based navigation system for mobile robot: a technological review," *Periodicals of Engineering and Natural Sciences*, vol.6, no.2, pp. 47-57, 2018.
- [7] K. Konolige, J. Augenbraun, N. Donaldson, C. Fiebig, P. Shah, "A low-cost laser distance sensor," in *Proc. IEEE International Conference on Robotics and Automation*, pp. 3002-3008, 2008.
- [8] X. Jin, J. Jung, S. Ko, E. Choi, J. O. Park, C. S. Kim, "Geometric parameter calibration for a cable-driven parallel robot based on a single one-dimensional laser distance sensor measurement and experimental modeling," *Sensors*, vol. 18, no. 7, pp. 2392, 2018.
- [9] N. Y. Ko and T. Y. Kuc, "Fusing range measurements from ultrasonic beacons and a laser range finder for localization of a mobile robot," *Sensors*, vol. 15, no. 5, pp. 11050-11075, 2015.
- [10] R. Lange, "3D time-of-flight distance measurement with custom solid-state image sensors in CMOS/CCD-technology," Department of Electrical Engineering and Computer Science at University of Siegen, ch. 2, 2000.
- [11] G. Benet, F. Blanes, J. E. Simó, P. Pérez, "Using infrared sensors for distance measurement in mobile robots," *Robotics and Autonomous Systems*, vol. 40, no. 4, pp. 255-266, 2002.
- [12] Pololu 2490 - VL53L0X datasheet - [Online]. Available: <https://www.pololu.com/file/0J1187/vl53l0x.pdf>
- [13] Pololu 2489 - VL6180X datasheet - [Online]. Available: <https://www.pololu.com/file/0J961/vl6180x.pdf>
- [14] Pololu 2489 - VL6180X photo -[Online]. Available: <https://a.pololu-files.com/picture/0J6783.600x480.jpg?f14b5e870845363550254e8131ed7fd8>
- [15] Pololu 2490 - VL53L0X photo -[Online]. Available: <https://a.pololu-files.com/picture/0J7223.600x480.jpg?39275d0026d0809ee15839805229db3b>

Copyright © 2021 by the authors. This is an open access article distributed under the Creative Commons Attribution License ([CC BY-NC-ND 4.0](https://creativecommons.org/licenses/by-nc-nd/4.0/)), which permits the use, distribution and reproduction in any medium, provided that the article is properly cited, the use is non-commercial and no modifications or adaptations are made.

**Mateusz Świącki**, Wysokie Mazowieckie (Poland), July 2, 1998. Control System and Robotics student at the Białystok University of Technology. A student of the general high school named after King Kazimierz Jagiellończyk in Wysokie Mazowieckie, 2017.

**Józef Szymelewicz**, Szypliszki (Poland), May 14, 1998. Control System and Robotics student at the Białystok University of Technology. A student of the III. a general high school named after Alfred Lityński in Suwałki, 2017.

**Jerzy Matusiewicz**, Wizajny (Poland), 24 September 1998. Control System and Robotics student at the Białystok University of Technology. A student of the I. general high school named after Adam Mickiewicz in Białystok, 2017.

**Ph.D. Rafał Grądzki**, Mońki (Poland) December 22, 1984. In 2012 in Białystok University of Technology finished PhD thesis in technical sciences in the field of machine construction and operation. He works as assistant Professor of the Faculty of Mechanical Engineering at the Białystok University of Technology since 2012. Research subjects: technical diagnostics of bus engines, shafts, examination of potential reliability and safety level demonstrated by technical objects and autonomous robots. The most important publication 27. R. Grądzki, P. Z. Kulesza, B. Bartoszewicz, "Method of shaft crack detection based on squared gain of vibration amplitude", *Nonlinear Dynamics*, 2019, Volume 98, Issue 1, pp 671-690. <https://doi.org/10.1007/s11071-019-05221-0>.